

1 **Modeled and satellite-derived extreme wave height**
2 **statistics in the North Atlantic Ocean reaching 20 m**

3 **Kaushik Sasmal¹, Tsubasa Kodaira¹, Yuki Kita², Rei Miratsu³, Tingyao Zhu³,**
4 **Tsutomu Fukui³, Takuji Waseda¹**

5 ¹Graduate School of Frontier Sciences, The University of Tokyo, Kashiwa, Chiba, Japan

6 ²MS&AD InterRisk Research & Consulting, Inc., Chiyoda, Tokyo, Japan

7 ³Nippon Kaiji Kyokai (ClassNK), Chiyoda, Tokyo, Japan

8 **Key Points:**

- 9 • The wave height statistics reaching 20 m were derived from 25-year wave hindcast
10 and satellite-altimeter
11 • Inter-comparison of model, buoy and satellite revealed that uncertainty of satellite
12 altimeter reaches a few meters.
13 • The 25-year wave statistics is dominated by a single event in 2014.

Abstract

Wave statistics of the North Atlantic Ocean, instrumental in designing merchant ships, were revisited by an in-house high-resolution 25-year wave hindcast (TodaiWW3-NK). The tail of the exceedance probability of H_s was extended to 20 m and compared surprisingly well against the satellite altimeter. Moreover, we have found that the largest storm event in 25 years with the highest wave over 21 m in January 2014 significantly enhanced the tail of the H_s distribution, which is a feature that was common among the three wave-hindcasts (ERA5/ECMWF, IOWAGA/IFREMER, and TodaiWW3-NK). Paradoxically, the satellite altimeter did not detect the H_s at the peak of this storm. We found that extreme wave heights from models and satellites of three storms in 2007, 2011, and 2014 may deviate about a few meters among the estimates, particularly the altimeter having a large uncertainty. In-situ observations of the extreme wave events are urgently in need.

Plain Language Summary

Sea states in the North Atlantic Ocean is considered to be the severest among the basins with large ship traffic. Traditionally, the wave statistics in the North Atlantic Ocean were used to estimate the design loads of the ships. In this study, the wave statistics was reproduced based on numerical wave simulation of 1994 to 2018. The result was compared to the wave heights observed by satellites. They compare well up to almost 20 m wave height. However, we have found that the severest storm in 25 years registering 21 m and higher waves were not observed by satellites. This puzzling fact implies that the uncertainty of the satellite observation of the extreme wave events is large and has never been validated. We suggest enhancement of the in-situ observation of the extreme wave events.

1 Introduction

The sea states in the North Atlantic Ocean is considered to be the most severe among seas with heavy ship traffic. Therefore, the joint probability distribution of significant wave height (H_s) and wave period (T_z) (also referred to as scatter diagram) in the North Atlantic Ocean have been used to estimate wave loads which is a crucial factor for the structural design of ships (Cardone et al., 2015; Bitner-Gregersen et al., 2016). The scatter diagram is constructed based on ocean areas 8, 9, 15, and 16 of the Global Wave Statistics (GWS Hogben et al. (1986)) as recommended by the International Association of Classification Societies (IACS) Rec. 34, (see IACS. (2001)). The GWS database was derived from visual observations and may not include extreme wave heights caused by storms as the ships may have avoided navigating into the storms. Therefore, the existing GWS database does not represent extreme wave heights and the bias towards lower wave heights is corrected (Bitner-Gregersen et al., 2016).

In a recent study, a 23-year (1990-2012) hindcast dataset IOWAGA/IFREMER (Rascle & Ardhuin, 2013) was used to identify extreme wave regions in the North Atlantic Ocean by deriving spatial distribution of return periods of storms for a given H_s threshold value (Ponce de León et al., 2015). They found that the regions of extreme waves are associated with the storm tracks of tropical and extratropical cyclones. The North Atlantic Ocean experiences severe storms particularly during the winter months (December, January and February). Studies show that significant wave height (H_s) reached 20.0 m during several extreme events associated with rapidly intensifying extratropical cyclones (Cardone et al., 2011). The number of extratropical storms with hurricane force winds in the North Atlantic Ocean can exceed 10 per year (Hanafin et al., 2012).

There are two renowned extreme events observed by satellite altimeter. During an extreme event in 2011, the JASON-2 altimeter measured $H_s = 20.12$ m on February 14 at 11:03:09 UTC under the storm Quirin. This was "a record-breaking maximum value of H_s " according to Ardhuin et al. (2011). During another extreme event in 2007, the JASON-1

63 Ku-band altimeter measured H_s of 20.2 m on February 9, 2007, at 21:31 UTC (Cardone et
 64 al., 2009), which was reprocessed in NASA and CNES data to be 19.13 m (Ardhuin et al.,
 65 2011).

66 Within the 25-year analysis period (1994-2018) of our study, we found that a phenom-
 67 enal storm occurred in the North Atlantic Ocean during January 4-6, 2014. The name
 68 Hércules (Ponce De León & Guedes Soares, 2015b) was given to this winter storm because
 69 of its unusual size and intensity. It is noteworthy that none of the four satellite altimeters
 70 (JASON-2, HY-2A, CRYOSAT-2, SARAL) operating at that time captured the extreme
 71 waves at the peak of the storm intensification. The JASON-2 altimeter, which has a repeat
 72 cycle of 10-day measured only up to $H_s = 15.5$ m, whereas SARAL recorded $H_s = 19.24$ m.
 73 However, none of these altimeter passes were close to the core of the storm. Therefore, the
 74 H_s extreme under Hércules is undetected by the altimeters.

75 The wave heights during extreme events are undetected not only by altimeters but
 76 by buoys as well (Alves & Young, 2003). Nevertheless, three large wave events were de-
 77 tected by the moored buoy network of the UK Met Office. At the K3 buoy (53.52° N,
 78 18.46° W), H_s exceeding 18.0 m was registered during December 8-9 in 2007, and at the
 79 K2 buoy (51.00° N, 13.35° W), waves over 17.0 m H_s was registered on March 10, 2008
 80 (Turton & Fenna, 2008). During another extreme event in 2013, the K5 buoy recorded a
 81 H_s of 19.0 m at 0600 UTC on February 4th, 2013 in the North Atlantic Ocean (59.11° N,
 82 11.70° W). 19.0 m is the highest significant wave height measured by a buoy, according
 83 to WMO (<https://public.wmo.int/en/media/press-release/19-meter-wave-sets-new-record-highest-significant-wave-height-measured-buoy>). We present model validation for this ex-
 84 treme event by comparing two different hindcast datasets ERA5/ECWAM (Hersbach et
 85 al., 2020) and TodayWW3-NK. The model validation for such H_s extremes has not been
 86 reported before.
 87

88 In this paper, we revisit the wave statistics of GWS 8, 9, 15, and 16 areas in the
 89 North Atlantic Ocean by utilizing 25-year (1994-2018) wave hindcast data from our in-
 90 house TodayWW3-NK. Our objective is to re-derive the marginal distribution of H_s in
 91 the GWS 8, 9, 15, and 16 areas from TodayWW3-NK. The exceedance probability of H_s
 92 from TodayWW3-NK is validated against satellite altimeter data and compared against
 93 other models, ERA5/ECMWF, and IOWAGA/IFREMER. The TodayWW3-NK has the
 94 highest spatial and spectral resolutions. We demonstrate that the impact of one single storm
 95 event (January 2014) on 25-year wave statistics is outstanding and dominantly affects the
 96 distribution. We show a comparison of H_s among different wave datasets and observations
 97 from both altimeters and buoy during a few selected extreme events in the North Atlantic
 98 Ocean. In addition to this, we compare H_s during extreme events among satellite altimeter
 99 datasets obtained from different sources to highlight how the estimates deviate for the
 100 extremes.

101 2 Data and Methodology

102 We analyzed 25 years of reanalysis (ERA5) and hindcast (IOWAGA and TodayWW3-
 103 NK) data for GWS 8, 9, 15 and 16 areas (Figure S1). TodayWW3-NK model computational
 104 domain encompasses the Atlantic Ocean with the spatial resolution of $0.20^\circ \times 0.25^\circ$ (Lat
 105 \times Lon), 35 frequency bins and 36 directional bins. For model physics, the ST4 package of
 106 Ardhuin et al. (2010) was used. The model was forced by NCEP/CFSR hourly wind ((Saha
 107 et al., 2010, 2014)) and was integrated for 25 years in hindcast mode (1994-2018).

108 The spatial resolutions of ERA5 and IOWAGA are $0.36^\circ \times 0.36^\circ$ and $0.5^\circ \times 0.5^\circ$, re-
 109 spectively. The spectral resolution of ERA5 and IOWAGA are 24 directional bins and 30
 110 frequency bins, and 24 directional bins and 31 frequency bins, respectively. For IOWAGA,
 111 the WAVEWATCH III model was forced by either ECMWF or CFSR winds depending on
 112 the year. The ST4 physics (Ardhuin et al., 2010) is employed in which the wind-wave growth

113 parameter β_{max} was adjusted for different wind products to correct the average to higher
 114 wave heights (Ardhuin et al., 2011); $\beta_{max} = 1.52$ for ECMWF winds and $\beta_{max} = 1.33$ for
 115 CFSR winds.

116 For IOWAGA, no assimilation of the observed data was made, however, the model
 117 parameters were calibrated based on observations from buoys, satellite altimeters, SAR,
 118 and seismic noise spectra for years after 2008 (Ardhuin et al., 2011). For TodaiWW3-NK,
 119 no assimilation of observed data was made in the WAVEWATCH III model. The model was
 120 configured with ST4 physics package and forced by CFSR winds (Saha et al., 2010, 2014)
 121 with $\beta_{max} = 1.33$. The wave data in ERA5 were derived from ECWAM, which was forced
 122 by the winds from the ECMWF’s coupled model system (IFS). Satellite altimeter data are
 123 assimilated in ERA5 for correction of H_s .

124 The exceedance probability was calculated as $r/(n + 1)$ based on the 25 years H_s data,
 125 where r is the rank, and n is the total number of data. We used this method to calculate the
 126 exceedance probability of H_s from satellite altimeter data as well. Here, we used the satellite
 127 altimeter data of Ribal and Young (2019); 33 years (1985-2018) of satellite data from 13
 128 altimeters have been calibrated and quality controlled. They performed cross-calibration of
 129 H_s between different altimeters up to $H_s = 10.0$ m but did not guarantee the performance
 130 for the waves with $H_s > 10.0$ m. Upon comparing the exceedance probability between
 131 models and observations, we separated the altimeter data into two groups based on their
 132 repeat cycle; the altimeters with a repeat cycle of 10 days (TOPEX, JASON-1, JASON-2,
 133 and JASON-3) and the altimeters with a repeat cycle greater than or equal to 25 days
 134 (ERS-2, ENVISAT, CRYOSAT-2, SARAL, and SENTINEL-3A).

135 3 Results and Discussion

136 3.1 Exceedance probability of H_s from model and altimeter up to 20 m

137 Exceedance probabilities of H_s are estimated from the wave models and satellite alti-
 138 timer data. The H_s data extracted from altimeters with a 10-day repeat cycle agree
 139 surprisingly well with TodaiWW3-NK data to approximately 18.5 m (Figure 1a). The tails
 140 of both distributions reach over 20 m, considerably extending the wave statistics from 16 m
 141 derived from visual observation in the GWS 8, 9, 15, and 16 regions. In this comparison, the
 142 coincidence of the satellite measurements and the model estimates are neglected. Therefore,
 143 tracks of TOPEX, JASON-1, JASON-2, and JASON-3 located within GWS 8, 9, 15, and
 144 16 were all included. That is equivalent to applying an ergodic hypothesis in both space
 145 and time.

146 The reason why we used only the TOPEX, JASON-1, JASON-2, and JASON-3 derived
 147 H_s is because the altimeters with a 10-day repeat cycle are likely to capture more extremes
 148 compared to that with repeat cycle ≥ 25 days. The altimeter based distributions deviate
 149 from one another for $H_s > 7.0 - 8.0$ m (Figure S2). The tails of the distributions differ by
 150 more than 1.0 m between these two altimeter datasets. This comparison indicates that the
 151 H_s extremes (e.g., $H_s > 19.0$ m) might have gone undetected by the altimeters with repeat
 152 cycle ≥ 25 days due to under-sampling. Therefore, the higher sampling of altimeters with
 153 repeat cycle =10 days is the reason the altimeter derived H_s shows good agreement with
 154 that of the high-resolution model TodaiWW3-NK (Figure 1a).

155 The comparison of the exceedance probabilities of TodaiWW3-NK and satellite altime-
 156 ter derived H_s is encouraging, but the comparison neglects the coincidence of the observa-
 157 tion. It is anticipated that the locations and timings of the storm events have phase shifts,
 158 and therefore, the collocated observations may not match. From the collocated comparison
 159 of TodaiWW3-NK and altimeter derived H_s along satellite tracks of TOPEX, JASON-1,
 160 JASON-2, and JASON-3, we have found that the altimeter data tend to overestimate the H_s
 161 over 15.0 m. The conjecture derives from the inspection of a Q-Q plot and the correspond-
 162 ing exceedance probabilities of H_s (Figure S3). Overall, the correlation is 0.97, with almost

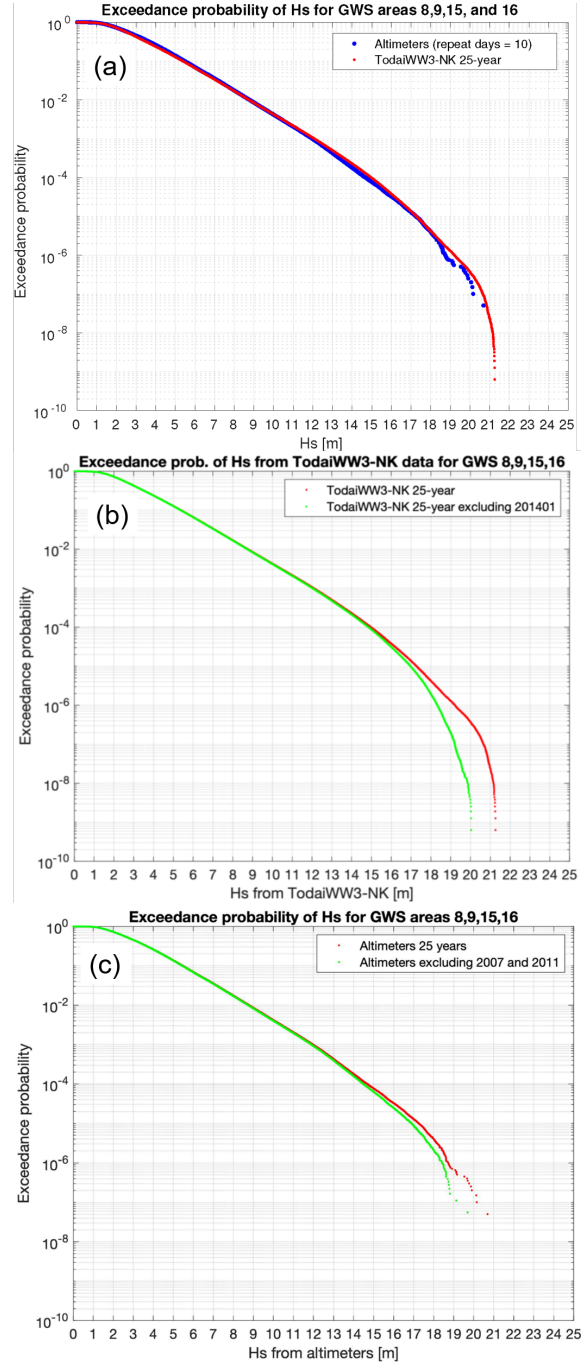


Figure 1. (a) Comparison of exceedance probability of significant wave height between model and altimeters. The altimeters with repeat days = 10 are TOPEX, JASON-1, JASON-2, and JASON-3. The comparison is made for GWS areas 8,9,15 and 16 using 25 years data from 1994 to 2018. The vertical axis is in log scale and the horizontal axis is in linear scale. (b) Exceedance probability of H_s from TodaiWW3-NK using 25 year 3-hourly data from 1994 to 2018 for GWS areas 8, 9, 15 and 16. The exceedance probability of H_s is compared with and without January 2014 data. (c) Exceedance probability of H_s from JASON-2 are compared using 25 year records from 1994 to 2018 within GWS areas 8, 9, 15 and 16, with and without 2014 and 2017 storm data.

163 negligible bias, root-mean-squared-error (RMSE) of 0.45 m, and a scatter index (SI) of 0.14,
 164 but they start to deviated beyond $H_s = 15.0$ m. Moreover, the tails of the distributions are
 165 quite different for $H_s > 19.0$ m.

166 Nevertheless, the agreement of wave model and satellite altimetry up to 15 m H_s is
 167 remarkable as altimeter-derived H_s has only been validated up to 10 m or so (Ribal &
 168 Young, 2019). The model is not perfect. However, we conclude that the spatial and spectral
 169 resolutions of the model are key parameters affecting the reproducibility of the extreme
 170 wave events, and, therefore, the TodaiWW3-NK is a suitable model to study the wave ex-
 171 tremes. The exceedance probabilities from the three independent models were compared.
 172 For example, the values of H_s at exceedance probability of 10^{-8} are roughly 19.8 m, 20.3 m,
 173 and 21.1 m from ERA5, IOWAGA, and TodaiWW3-NK, respectively (Figure S4). Consid-
 174 ering that the only difference between TodaiWW3-NK and IOWAGA is the spatial and the
 175 spectral resolutions (see section 2), and neither the model physics nor the wind forcing, we
 176 may conclude that the TodaiWW3-NK with higher spatial resolution produced higher H_s
 177 than that of IOWAGA. ERA5/ECWAM largely underestimates the wave height, despite its
 178 native spatial resolution of $0.36^\circ \times 0.36^\circ$, and assimilation of satellite altimeter data.

179 In summary, we have discovered that the exceedance probabilities of H_s derived from
 180 TodaiWW3-NK and satellite-altimeter agree quite well up to 19 m or so. However, their
 181 collocated comparison starts to deteriorate beyond 15 m. The disagreement is partly because
 182 we rarely observe extreme wave events over 15 m. In the following, we will study in-depth
 183 the selected historical extreme events.

184 3.2 Extreme event in January 2014

185 The North Atlantic Ocean experienced several distinct 10-year return period storms
 186 during the 2013-2014 winter (Castelle et al., 2015), but the storm that formed during Jan-
 187 uary 4-6 was extraordinary. Hércules was an unprecedented storm covering almost the entire
 188 North Atlantic Ocean (Ponce De León & Guedes Soares, 2015b). By definition, Hércules is
 189 an explosive cyclone (Sanders & Gyakum, 1980), as the SLP dropped 38 hPa within 24 h;
 190 from 971 hPa at 00:00 UTC 04 Jan to 933 hPa, according to NOAA OPC synoptic maps
 191 (Figure S5 a,c). Extraordinary large swells reached the Iberian Peninsula causing devastat-
 192 ing damage to the coastal region in France (Castelle et al., 2015) and in Portugal (Silva et
 193 al., 2017).

194 The spatial distribution of H_s at 2014.1.5 06:00 UTC from TodaiWW3-NK is shown
 195 in Figure 2a. The maximum significant wave height ($H_{s,max} = 21.26$ m) is attained at the
 196 south of the minimum SLP point and west of the warm front (Figure 2b), consistent with
 197 the depiction of the explosive cyclones in the Pacific Ocean (Kita et al., 2018). The area
 198 with high wave height also corresponds to where the directional spectrum narrows.

199 This extraordinary event in January 2014 exhibited a remarkable effect on the 25-year
 200 wave statistics. The comparison of the exceedance probabilities of H_s with and without the
 201 2014.1 data revealed that this single event significantly enhanced the tail of the distribution
 202 (Figure 1b). When the 2014.1 data were excluded from the analysis, the largest H_s did not
 203 exceed 20.0 m. This means that the waves over 20 m H_s were associated only with the storm
 204 on January 4-6, 2014. We have also examined 25-year statistics from ERA5/ECMWF and
 205 IOWAGA/IFREMER, and both models unequivocally showed that the tail was enhanced
 206 by the January 2014 event (Figure S6).

207 Unquestionably, waves under Hércules is imperative in determining the 25-year North
 208 Atlantic wave statistics. However, it turns out that none of the satellite altimeters captured
 209 this event. JASON-2 is not an exception and missed the centre of the storm (Figure 2a). The
 210 highest H_s from the three models are 21.26 m, 20.43 m and 20.33 m from TodaiWW3-NK,
 211 IOWAGA, ERA5, respectively (Figures S7 a,c,e). However, even the JASON-2 track closest
 212 to the center largely underestimate the peak wave height under Hércules (Figures S7 b,d,f).

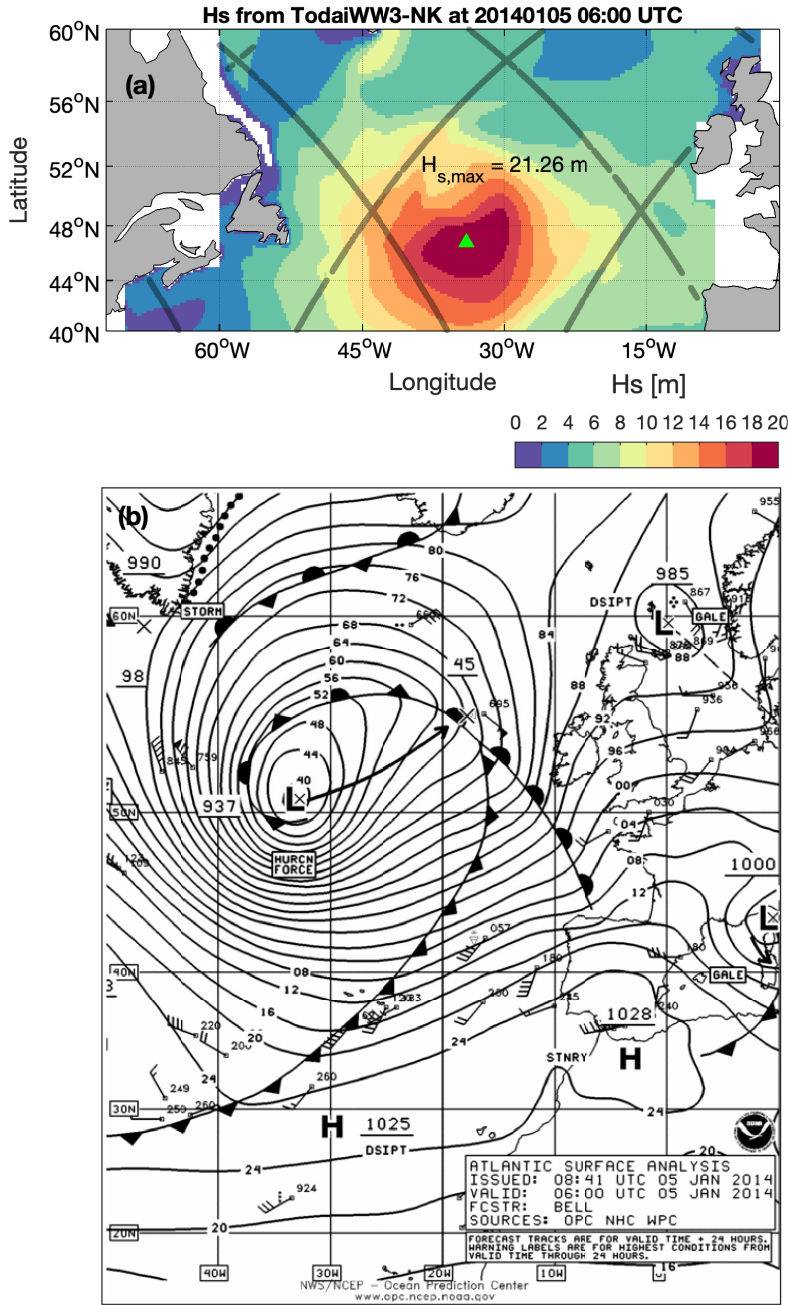


Figure 2. Spatial distribution of H_s from TodaiWW3-NK during the extreme event in January 2014. In subplot (a) the snapshot of H_s is shown for January 5, 2014 at 0600 UTC. The location of $H_{s,max}$ is highlighted by a green color triangle. The altimeter tracks of JASON-2 on January 5, 2014 are plotted on top of H_s . In subplot (b) NOAA OPC synoptic analysis charts is shown for 06:00 UTC on 05 Jan 2014.

213 The highest H_s from JASON-2 only went up to 15.5 m. We have scanned all the tracks
 214 of satellite altimeters that were operating during January 2014 and found that a segment
 215 of SARAL altimeter track passed closest to the center of the storm; the highest observed
 216 significant wave height reached $H_s = 19.24\text{m}$ at 48.20N, 29.42W, 20140105 07:23:22 UTC
 217 (Figures S7 g). Wave heights along this track were compared against the three independent
 218 hindcasts (Figures S7 h); both TodaiWW3-NK and IOWAGA seems to compare well with
 219 the altimeter derived data with a small bias, while ERA5 deviated by about 4 m at the
 220 storm peak and a large overall bias of -1.79 m (Table S1).

221 Satellites likely miss detecting the extreme waves under storms, and indeed the extreme
 222 waves under Hércules were not detected. As a consequence, removal of the 2014 data had
 223 hardly any effect on the satellite-derived 25-year exceedance probability. Then, why did
 224 the 25-year satellite-derived statistics compare well with the model (Figure 1a)?. Historical
 225 storms in the north Atlantic were identified and their impacts on the 25-year statistics were
 226 investigated. It turns out that the 2007 and 2011 storms contributed the most to enhance the
 227 tail of the satellite-derived distribution. By removing the two years from the statistics, the
 228 tail of the distribution reduced beyond 15 m, and underestimated the extremes compared to
 229 the full dataset (Figure 1c). Noting that these two storms were not as influential as the 2014
 230 storm, this result suggests that the satellite-derived extreme wave heights are erroneous. To
 231 that end, we will compare models to satellites with available collocated buoy observations
 232 for the 2007 and 2011 events in section 3.3.

233 Lastly, the biases of the wave models may originate from the wind. We compared
 234 the CFSv2 wind speed that was used to force TodaiWW3-NK with the satellite wind data
 235 (Figures S8-S10). The maximum wind speeds were 47.4 ms^{-1} , 50.0 ms^{-1} , and 39.6 ms^{-1} for
 236 ASCAT, WindSat2, and OceanSat2, respectively, and were mostly faster than the maximum
 237 wind speed from CFSv2, 41.2 ms^{-1} . Therefore, it is unlikely that the model overestimated
 238 the 2014 event. Satellite-based measurements are known to have errors at high wind speeds
 239 (Hanafin et al., 2012).

240 3.3 Comparison of wave hindcasts with 2007 and 2011 extreme events

241 Both model and satellite observations need validation of the extremes. This is the lesson
 242 from the comparison of models and satellite observations of the January 2014 event. Here we
 243 analyze satellite altimeter data during the 2007 and 2011 extreme events when the JASON
 244 tracks were close to the storm center and registered H_s exceeding 20.0 m. The JASON-
 245 1 altimeter measured $H_s=20.0$ m during 9th February 2007 and the JASON-2 measured
 246 $H_s=20.1$ m on 14 February 2011 during the storm Quirin (Figures 3a,b). The H_s from
 247 TodaiWW3-NK, IOWAGA, and ERA5 are compared with the altimeter data (Figures 3c,d).
 248 The ERA5 consistently shows the lowest wave height while the TodaiWW3-NK shows the
 249 highest (Figures 3c,d). In the case of 2007 event, TodaiWW3-NK and IOWAGA compared
 250 well with the satellite, and in the case of 2011 event, IOWAGA tended to show lower wave
 251 heights than TodaiWW3-NK. Overall, TodaiWW3-NK reproduced the H_s well except at the
 252 peak of the event. This is attributed to the higher spatial resolution $0.20^\circ \times 0.25^\circ$ (Latitude
 253 \times Longitude) of TodaiWW3-NK compared to IOWAGA and ERA5. Results from these
 254 analyses indicate that higher spatial resolution of the model plays an important role to
 255 capture wave heights during an extreme event.

256 Previous studies of the extreme events in 2007 and 2011 showed that the model repro-
 257 duced high waves up to $H_s=20.0$ m, but provided that the wind forcing was tuned (Cardone
 258 et al., 2009; Ardhuin et al., 2011; Hanafin et al., 2012; Ponce De León & Guedes Soares,
 259 2015a, 2015b). For the storm in February 2007, a WAM model simulation forced by CFSR
 260 wind agreed well with the JASON-1 along-track data, although the model slightly overesti-
 261 mated the H_s at the peak (Ponce de León & Guedes Soares, 2014). For the extreme event
 262 in February 2011, when the NCEP wind speed was increased by 10 %, the modeled H_s
 263 showed good agreement with JASON-2 along-track data (Ardhuin et al., 2011; Hanafin et

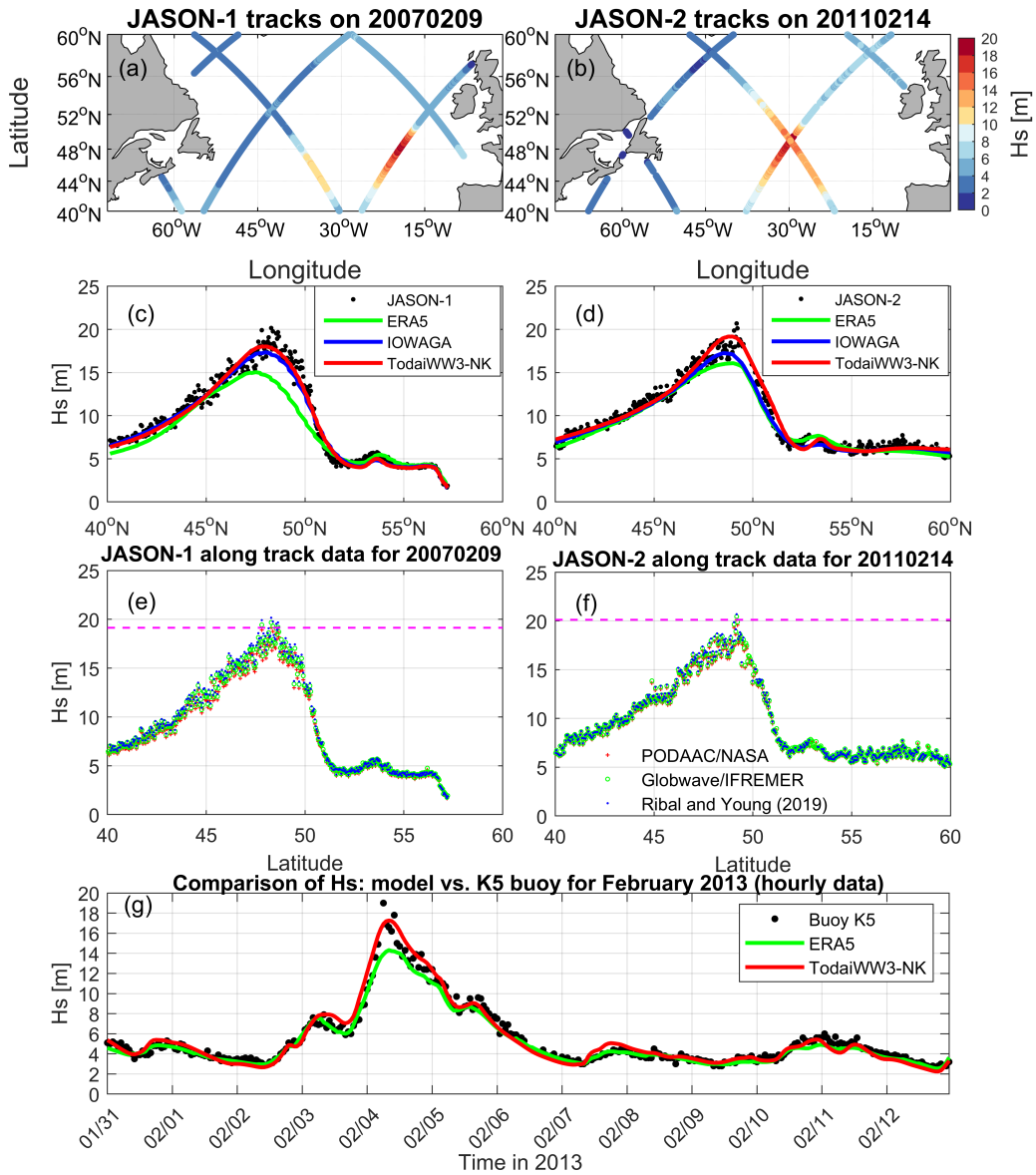


Figure 3. Significant wave height along JASON-1 tracks on February 9th 2007 and JASON-2 tracks on February 14th 2011 are shown in (a) and (b). Comparison of models against altimeter along track data are shown in subplots (c) and (d). Satellite altimeter products from PODAAC/NASA, Globwave/IFREMER, and Ribal and Young (2019), are compared for: (e) the extreme event on February 9, 2007, from the JASON-1; (f) the extreme event on February 14, 2011, from the JASON-2. In subplot (g), a comparison of significant wave heights between models and buoy observations are presented for the extreme event in February 2013. The time-series of hourly H_s data from UK Met Office buoy K5 and models are compared. The IOWAGA data is not included in this comparison as it is 3-hourly data.

264 al., 2012). Whereas, in *TodaiWW3-NK*, the value of wind-wave growth parameter of the
 265 *ST4* model physics was tuned to $\beta_{max} = 1.33$ (CFSR wind forcing), which is consistent with
 266 *IOWAGA*.

267 However, validating the model against one satellite product is not the end of the story.
 268 It turns out that different satellite H_s products produce a large deviation in their estimates.
 269 For these two extreme events, we compared different *JASON-1* and *JASON-2* altimeter prod-
 270 ucts obtained from Ribal and Young (2019) (RY), *Globwave* (GW), and *PODAAC/NASA*
 271 (PN) (Figure 3e,f). For $H_s < 10$ m, altimeter products compare well, however for H_s beyond
 272 10-12 m, the altimeter products start to scatter as much as a few meters and deviate among
 273 them. For the extreme event in February 2007, the maximum H_s from RY, GW, and PN
 274 are 20.16 m, 19.67 m, and 19.13 m, respectively. Whereas during the extreme event in
 275 February 2011, the maximum H_s from RY, GW, and PN are 20.69 m, 20.44 m, and 20.12
 276 m, respectively. Overall, H_s from RY was the largest, and H_s from PN was the smallest,
 277 with a bias of around 0.4 m. Despite derived from identical satellite altimeter, the H_s from
 278 different sources show deviation because the algorithm used to derive them are different.
 279 Finally, we conjecture that the bias and the large intermittency of the satellite-derived H_s
 280 may have contributed to the overestimation of the 2007 and 2011 extreme events. As a
 281 result, the tail of the exceedance probability was erroneously enhanced (Figure 1c).

282 3.4 The highest H_s as measured by a buoy in 2013

283 Finally, this section illustrates the significance of in-situ observation. None of the
 284 extreme events in 2007, 2011, and 2014 studied in this paper were registered by in-situ
 285 observations. Historically, no buoys had observed waves higher than 20 m. The largest wave
 286 height registered by a buoy is 19.0 m from the UK Met Office (K5 buoy) during an extreme
 287 event in Feb 2013. The record was examined by the World Meteorological Organization
 288 expert committee and was reported as "the highest significant wave height as measured by
 289 a buoy." Here we present a comparison of the buoy observation with hourly data from *ERA5*
 290 and *TodaiWW3-NK* (Figure 3g). As aforementioned, *ERA5* underestimates the extreme,
 291 whereas *TodaiWW3-NK* mostly follows the rapid increase of H_s . We also note a spiky nature
 292 of the buoy estimated H_s ; the 19 m H_s rapidly drops to around 17 m or less for the following
 293 3 hours, and then increases again to 18 m or so, immediately followed by a drop to 15 m
 294 or less. We may attribute such intermittency of the in-situ observation to the sampling
 295 variability or by the intrinsic variability not resolved by the model (Bitner-Gregersen &
 296 Magnusson, 2014). Besides, the accelerometer-based buoy observation may require special
 297 attention in detecting extremes (Collins et al., 2014). As such, the in-situ data itself needs
 298 to be validated at the extreme event. More in-situ observations are necessary.

299 4 Summary and Conclusions

300 In this paper we have revisited the wave statistics of the GWS 8,9,15,16 areas in the
 301 North Atlantic Ocean by analyzing 25 years of hindcast and reanalysis wave data from
 302 *ERA5*, *IOWAGA*, and *TodaiWW3-NK*. The *TodaiWW3-NK* based exceedance probability
 303 of H_s compared well with altimeter-derived data up to almost 20.0 m. Within the 25 years
 304 (1994-2018), the maximum value of H_s exceeded 21.0 m from *TodaiWW3-NK* during the
 305 storm *Hercules* in January 4-6, 2014. The impact of this single storm on 25-year wave statis-
 306 tics is noteworthy as it significantly enhanced the tail of H_s distribution. The comparison
 307 of H_s between models and altimeter data for three extreme events reveal that the tail of the
 308 distribution was most enhanced with *TodaiWW3-NK*, slightly less enhanced with *IOWAGA*
 309 and largely reduced with *ERA5*. The difference of the first two is attributed to the difference
 310 in their spatial resolutions.

311 The finding that the H_s at the peak of the 2014 storm was not detected by *JASON-2*
 312 was unanticipated and suggests that the 25-year altimeter derived statistics is indepen-
 313 dent of this event. Since the three independent models unequivocally demonstrated the

314 anomalous impact of the 2014 storm, we then conjectured that the extreme waves detected
 315 by satellite altimeter have large uncertainty. Moreover, for the extreme wave heights, the
 316 JASON-2 derived H_s products largely differed among the estimates (PODAAC/NASA,
 317 Globwave/IFREMER, Ribal and Young, 2019). Besides, altimeters have their limitation in
 318 providing a spatial coverage as the H_s is measured along the tracks only. Therefore, the
 319 extreme events may not be fully detected by altimeters due to under-sampling. To achieve
 320 a better spatial coverage of H_s during an extreme event such as a storm, altimeters with
 321 higher sampling will be useful (i.e., repeat cycle less than 10 days). The satellite altimeter
 322 data have never been calibrated for the extremes, and we expect that the cross calibration
 323 of H_s (e.g. Ribal and Young 2019) will be performed for H_s beyond 10 m in the future.

324 In-situ wave measurements during extreme events are essential for the calibration of
 325 altimeter data and validation of model results. However, there are no in-situ wave measure-
 326 ments available in the open water of the North Atlantic Ocean. In the past, the moored
 327 buoy network of UK Met Office measured H_s up to 18.0-19.0 m, although these buoys are
 328 not under the area of historical extreme wave events. More in-situ wave measurements are
 329 required in the open ocean during extreme events. Recently, the spotter buoy network in
 330 the Pacific Ocean started to provide valuable wave information with more than 150 spotter
 331 buoys. However, until now, there is no such buoy network in the North Atlantic Ocean.
 332 Therefore, a network of similar buoys in the North Atlantic Ocean, if deployed, will provide
 333 us a better insight of H_s during extreme events in the future.

334 Acknowledgments

335 The study presented in this paper was carried out within a joint research project between
 336 the University of Tokyo and Nippon Kaiji Kyokai (ClassNK).
 337 ERA5 data is available on the Copernicus Climate Change Service (C3S) Climate Data
 338 Store, and IOWAGA data is available from the IOWAGA-Ifremer data base. Their URLs
 339 are listed in the Supporting Information together with links to Ribal and Young (2019)
 340 data, Globwave altimeter data, PODAAC/NASA altimeter data, buoy data, Satellite winds
 341 (Widsat, ASCAT, OceanSat-2) and CFSR wind and sea ice concentration.

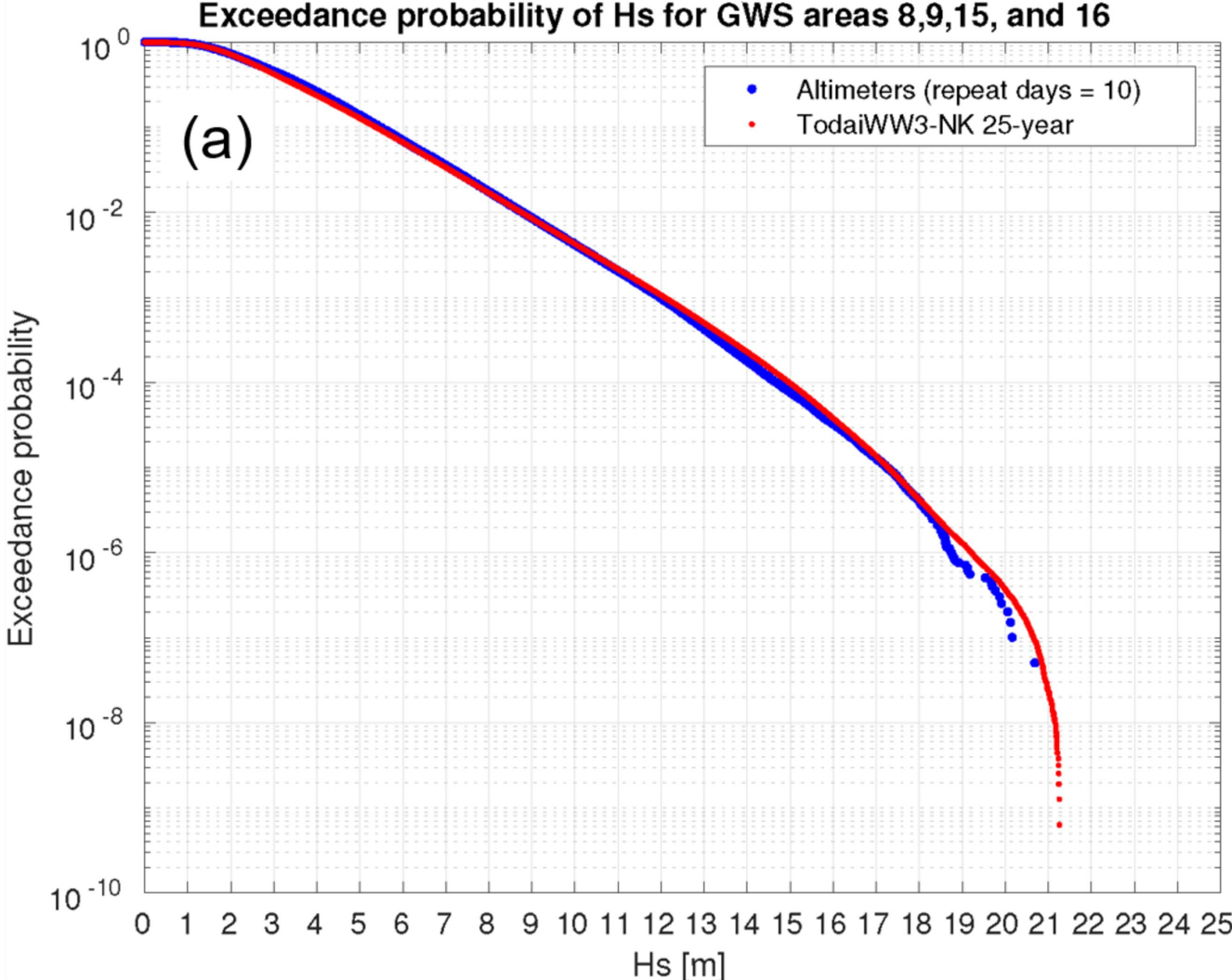
342 References

- 343 Alves, J. H. G., & Young, I. R. (2003). On estimating extreme wave heights using combined
 344 geosat, topex/poseidon and ers-1 altimeter data. *Applied Ocean Research*, *25*(4),
 345 167–186.
- 346 Ardhuin, F., Hanafin, J., Quilfen, Y., Chapron, B., Queffelec, P., Obrebski, M., . . . Van-
 347 demark, D. (2011). Calibration of the iowaga global wave hindcast (1991–2011) using
 348 ecmwf and cfsr winds. In *Proceedings of the 2011 international workshop on wave hind-*
 349 *casting and forecasting and 3rd coastal hazard symposium, kona, hi, usa* (Vol. 30).
- 350 Ardhuin, F., Rogers, E., Babanin, A. V., Filipot, J.-F., Magne, R., Roland, A., . . . others
 351 (2010). Semiempirical dissipation source functions for ocean waves. part i: Definition,
 352 calibration, and validation. *Journal of Physical Oceanography*, *40*(9), 1917–1941.
- 353 Bitner-Gregersen, E. M., Dong, S., Fu, T., Ma, N., Maisondieu, C., Miyake, R., & Rychlik,
 354 I. (2016). Sea state conditions for marine structures’ analysis and model tests. *Ocean*
 355 *Engineering*, *119*, 309–322.
- 356 Bitner-Gregersen, E. M., & Magnusson, A. K. (2014). Effect of intrinsic and sampling
 357 variability on wave parameters and wave statistics. *Ocean Dynamics*, *64*(11), 1643–
 358 1655.
- 359 Cardone, V., Callahan, B., Chen, H., Cox, A., Morrone, M., & Swail, V. (2015). Global
 360 distribution and risk to shipping of very extreme sea states (vess). *International*
 361 *Journal of Climatology*, *35*(1), 69–84.
- 362 Cardone, V., Cox, A., Morrone, M., & Swail, V. R. (2009). Satellite altimeter detection of
 363 global very extreme sea states (vess). In *Proc. 11th int. workshop on wave hindcasting*
 364 *and forecasting*.

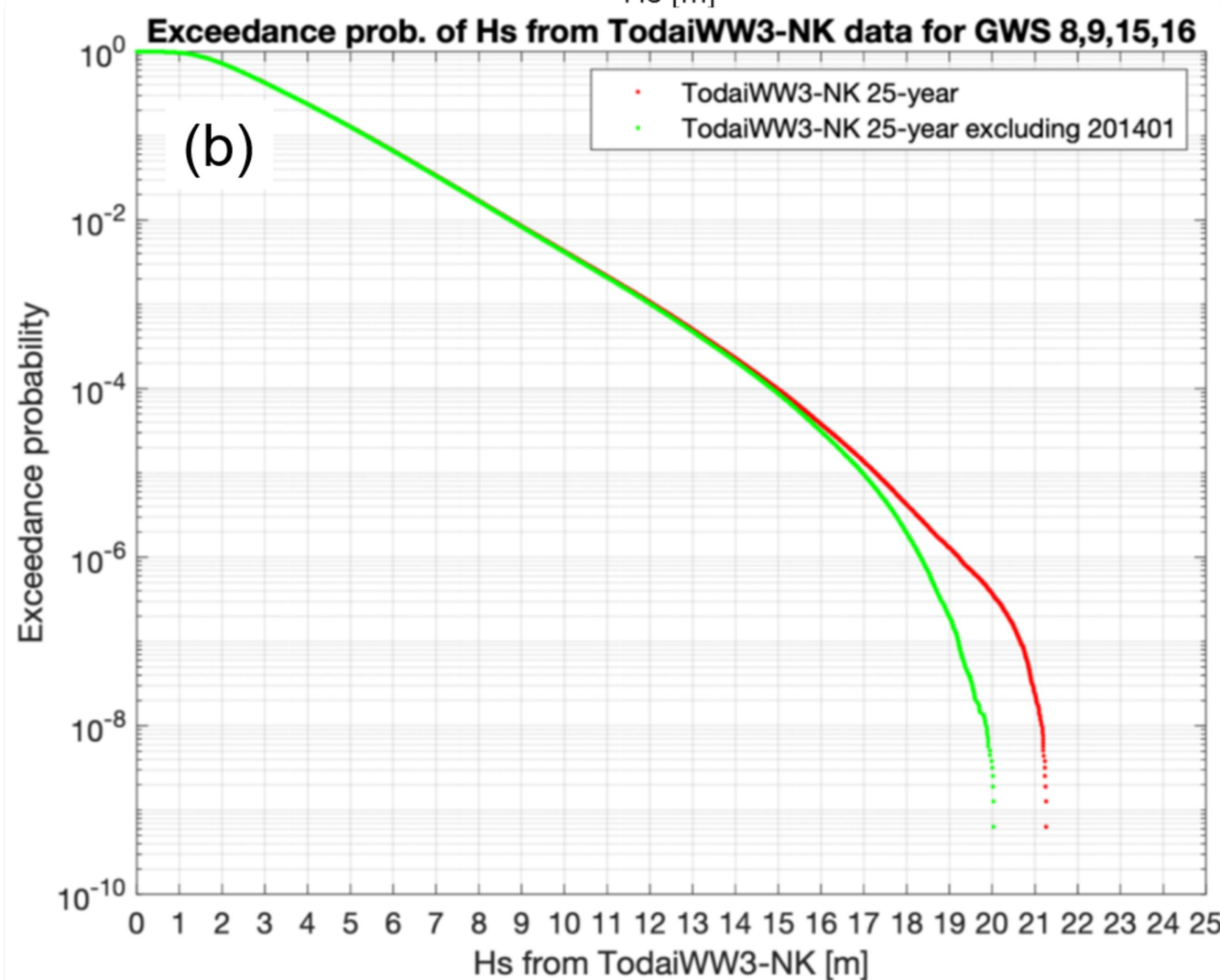
- 365 Cardone, V., Cox, A. T., Morrone, M. A., & Swail, V. R. (2011). Global distribution and
 366 associated synoptic climatology of very extreme sea states (vess). In *Proceedings 12th*
 367 *international workshop on wave hindcasting and forecasting, hawaii*.
- 368 Castelle, B., Mariou, V., Bujan, S., Splinter, K. D., Robinet, A., Sénéchal, N., & Ferreira,
 369 S. (2015). Impact of the winter 2013–2014 series of severe western europe storms
 370 on a double-barred sandy coast: Beach and dune erosion and megacusp embayments.
 371 *Geomorphology*, *238*, 135–148.
- 372 Collins, C. O., Lund, B., Waseda, T., & Graber, H. C. (2014). On recording sea surface
 373 elevation with accelerometer buoys: lessons from itop (2010). *Ocean Dynamics*, *64*(6),
 374 895–904.
- 375 Hanafin, J. A., Quilfen, Y., Arduin, F., Sienkiewicz, J., Queffeuilou, P., Obrebski, M.,
 376 ... others (2012). Phenomenal sea states and swell from a north atlantic storm in
 377 february 2011: a comprehensive analysis. *Bulletin of the American Meteorological*
 378 *Society*, *93*(12), 1825–1832.
- 379 Hersbach, H., Bell, B., Berrisford, P., Hirahara, S., Horányi, A., Muñoz-Sabater, J., ... oth-
 380 ers (2020). The era5 global reanalysis. *Quarterly Journal of the Royal Meteorological*
 381 *Society*.
- 382 Hogben, N., Da Cunha, L., & Oliver, H. (1986). Global Wave Statistics. *Unwin Brothers*
 383 *Limited London, England*.
- 384 IACS. (2001). International association of classification societies. Recommendation no. 34,
 385 standard wave data. <http://www.iacs.org.uk>.
- 386 Kita, Y., Waseda, T., & Webb, A. (2018). Development of waves under explosive cyclones
 387 in the northwestern pacific. *Ocean Dynamics*, *68*(10), 1403–1418.
- 388 Ponce de León, S., Bettencourt, J. H., Brennan, J., & Dias, F. (2015). Evolution of the ex-
 389 treme wave region in the north atlantic using a 23 year hindcast. In *International confe-*
 390 *rence on offshore mechanics and arctic engineering* (Vol. 56499, p. V003T02A019).
- 391 Ponce de León, S., & Guedes Soares, C. (2014). Extreme wave parameters under north
 392 atlantic extratropical cyclones. *Ocean Modelling*, *81*, 78–88.
- 393 Ponce De León, S., & Guedes Soares, C. (2015a). Hindcast of extreme sea states in north
 394 atlantic extratropical storms. *Ocean Dynamics*, *65*(2), 241–254.
- 395 Ponce De León, S., & Guedes Soares, C. (2015b). Hindcast of the hércules winter storm in
 396 the north atlantic. *Natural Hazards*, *78*(3), 1883–1897.
- 397 Rascle, N., & Arduin, F. (2013). A global wave parameter database for geophysical
 398 applications. part 2: Model validation with improved source term parameterization.
 399 *Ocean Modelling*, *70*, 174–188.
- 400 Ribal, A., & Young, I. R. (2019). 33 years of globally calibrated wave height and wind
 401 speed data based on altimeter observations. *Scientific data*, *6*(1), 1–15.
- 402 Saha, S., Moorthi, S., Pan, H.-L., Wu, X., Wang, J., Nadiga, S., ... others (2010). The
 403 NCEP climate forecast system reanalysis. *Bulletin of the American Meteorological*
 404 *Society*, *91*(8), 1015–1058.
- 405 Saha, S., Moorthi, S., Wu, X., Wang, J., Nadiga, S., Tripp, P., ... others (2014). The
 406 NCEP climate forecast system version 2. *Journal of Climate*, *27*(6), 2185–2208.
- 407 Sanders, F., & Gyakum, J. R. (1980). Synoptic-dynamic climatology of the bomb. *Monthly*
 408 *Weather Review*, *108*(10), 1589–1606.
- 409 Silva, S. F., Martinho, M., Capitão, R., Reis, T., Fortes, C. J., & Ferreira, J. C. (2017).
 410 An index-based method for coastal-flood risk assessment in low-lying areas (costa de
 411 caparica, portugal). *Ocean & Coastal Management*, *144*, 90–104.
- 412 Turton, J., & Fenna, P. (2008). Observations of extreme wave conditions in the north-east
 413 atlantic during december 2007. *Weather*, *63*(12), 352–355.

Figure 1.

Exceedance probability of Hs for GWS areas 8,9,15, and 16



Exceedance prob. of Hs from TodaiWW3-NK data for GWS 8,9,15,16



Exceedance probability of Hs for GWS areas 8,9,15,16

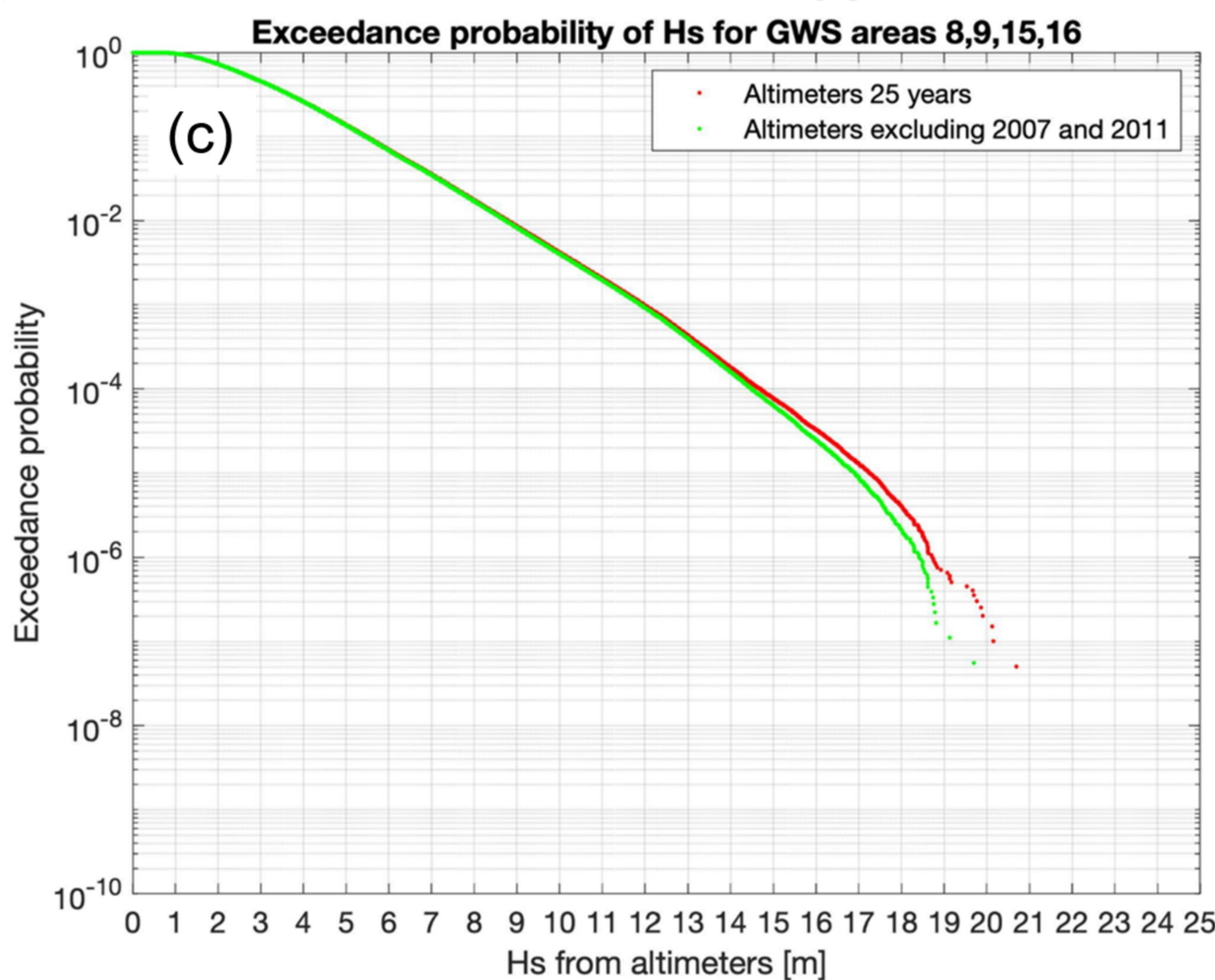


Figure 2.

Hs from TodaiWW3-NK at 20140105 06:00 UTC

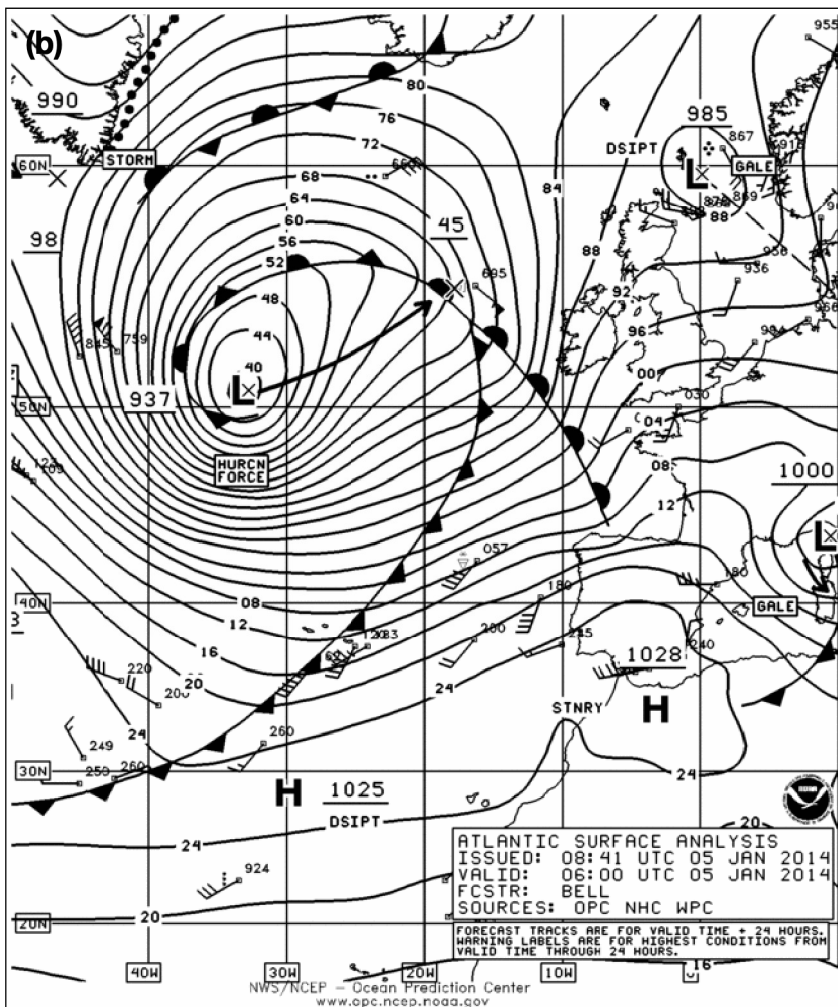
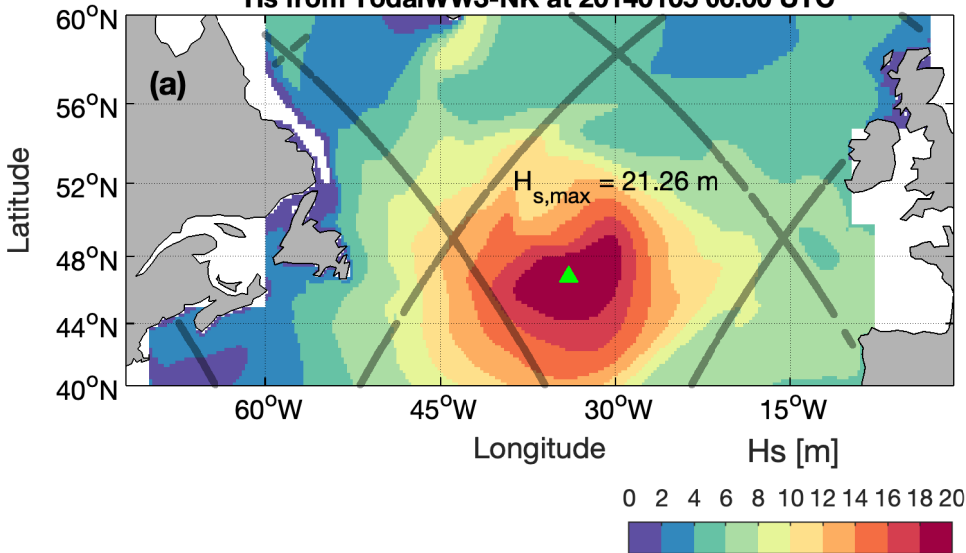


Figure 3.

